BAMS
Map Room

A Hydrometeorological Assessment of the Historic 2019 Flood of Nebraska, Iowa, and South Dakota

PAUL XAVIER FLANAGAN, REZAUL MAHMOOD, NATALIE A. UMPHLETT, ERIN HAACKER, C. RAY, WILLIAM SORENSEN, MARTHA SHULSKI, CRYSTAL J. STILES, DAVID PEARSON, AND PAUL FAJMAN

ABSTRACT: During early 2019, a series of events set the stage for devastating floods in eastern Nebraska, western Iowa, and southeastern South Dakota. When the floodwaters hit, dams and levees failed, cutting off towns while destroying roads, bridges, and rail lines, further exacerbating the crisis. Lives were lost and thousands of cattle were stranded. Estimates indicate that the cost of the flooding has topped $3 billion as of August 2019, with this number expected to rise. After a warm and wet start to winter, eastern Nebraska, western Iowa, and southeastern South Dakota endured anomalously low temperatures and record-breaking snowfall. By March 2019, rivers were frozen, frost depths were 60–90 cm, and the water equivalent of the snowpack was 30–100 mm. With these conditions in place, a record-breaking surface cyclone rapidly developed in Colorado and moved eastward, producing heavy rain toward the east and blizzard conditions toward the west. In areas of eastern Nebraska, western Iowa, and southeastern South Dakota, rapid melting of the snowpack due to this rain-on-snow event quickly led to excessive runoff that overwhelmed rivers and streams. These conditions brought the region to a standstill. In this paper, we provide an analysis of the antecedent conditions in eastern Nebraska, western Iowa, and southeastern South Dakota and the development of the surface cyclone that triggered the historic flooding, along with a look into the forecast and communication of flood impacts prior to the flood. The study used multiple datasets, including in situ observations and reanalysis data. Understanding the events that led to the flooding could aid in future forecasting efforts.

https://doi.org/10.1175/BAMS-D-19-0101.1
Corresponding author: Paul Flanagan, pflanagan3@unl.edu
In final form 26 February 2020

AFFILIATIONS: Flanagan, Mahmood, Umphlett, Sorensen, and Stiles—High Plains Regional Climate Center, and School of Natural Resources, University of Nebraska–Lincoln, Lincoln, Nebraska; **Haacker**—Department of Earth and Atmospheric Sciences, University of Nebraska–Lincoln, Lincoln, Nebraska; **Ray**—Nebraska Water Center, University of Nebraska–Lincoln, Lincoln, Nebraska; **Shulski**—School of Natural Resources, University of Nebraska–Lincoln, Lincoln, Nebraska; **Pearson and Fajman**—National Weather Service, Omaha, Nebraska

During the late winter season of 2019, a combination of anomalous events led to devastating floods across the central United States (Fig. 1). These events were punctuated by the passage of an extraordinarily deep surface cyclone that propagated across the region on 12–14 March. This storm system produced extreme weather, including blizzard conditions stretching from Colorado and Kansas through the Dakotas, and widespread liquid precipitation events in areas just to the east. Numerous daily precipitation records were broken, with some locations setting new records for highest 1-day precipitation for the month of March. Low pressure records over Colorado and Kansas were also broken. This flood event was exacerbated by the surface conditions across eastern Nebraska, western Iowa, and southeastern South Dakota (hereafter referred to as the study area), namely the widespread frozen or saturated soils, frozen rivers, and above-average river streamflow conditions (Fig. 2a) that led to numerous record river crests across the region (Figs. 2b–d and 9c). Initially, the excessive runoff overwhelmed smaller tributary rivers in the study area, which flow to larger rivers in the Platte and Missouri River basins. This resulted in failed levees and dams, leaving downriver locations overwhelmed with significant ice jams and water flow. This set of circumstances led to one of the most catastrophic flood events documented across the study

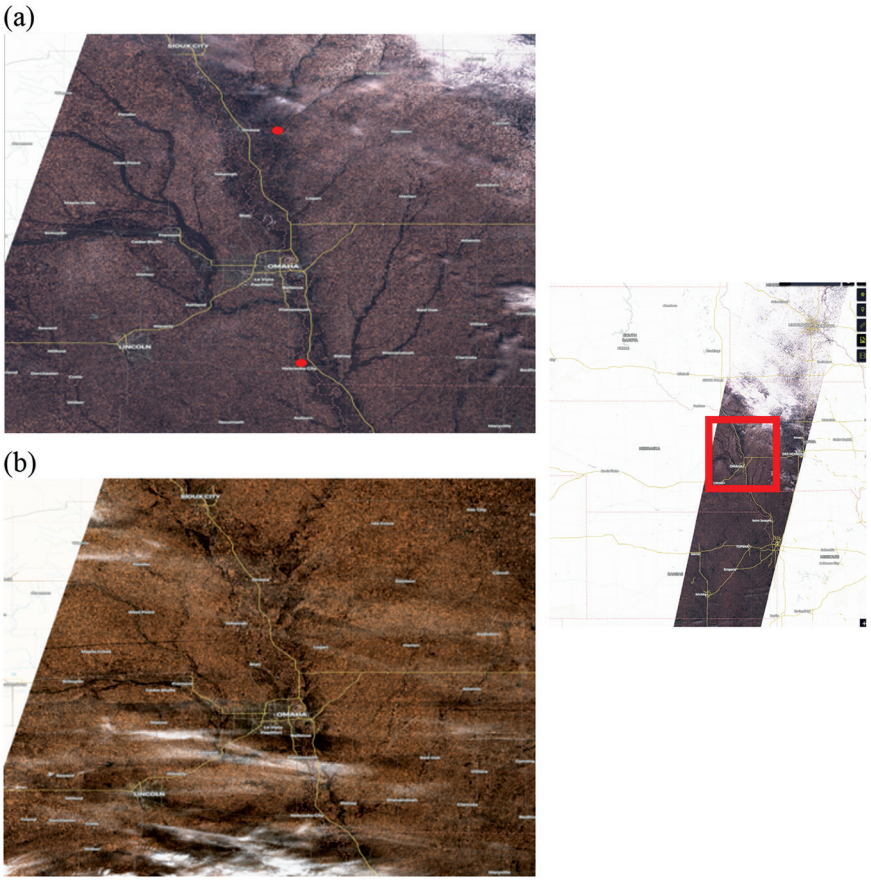

Fig. 1. (left) European Space Agency (ESA) (a) *Sentinel-2A* Level-1C visible-band satellite image on 16 Mar 2019. (b) *Sentinel-2A* Level-1C visible-band satellite image on 10 Jan 2019. (right) Also included is a zoomed-out image from 16 Mar 2019 showing the location of the zoomed-in area for (a) and (b). *Sentinel-2* images are taken from https://apps.sentinel-hub.com/eo-browser/?lat=40.2685&lng=-95.6738&zoom=10&time=2019-03-16&preset=1_TRUE_COLOR&datasource=Sentinel-2%20L2A**. The upper red dot in (a) represents the approximate location of the river gauge (Fig. 2c) in Turin, Iowa, and the lower red dot in (a) represents the approximate location of the river gauge (Fig. 2d) in Nebraska City, Nebraska.**

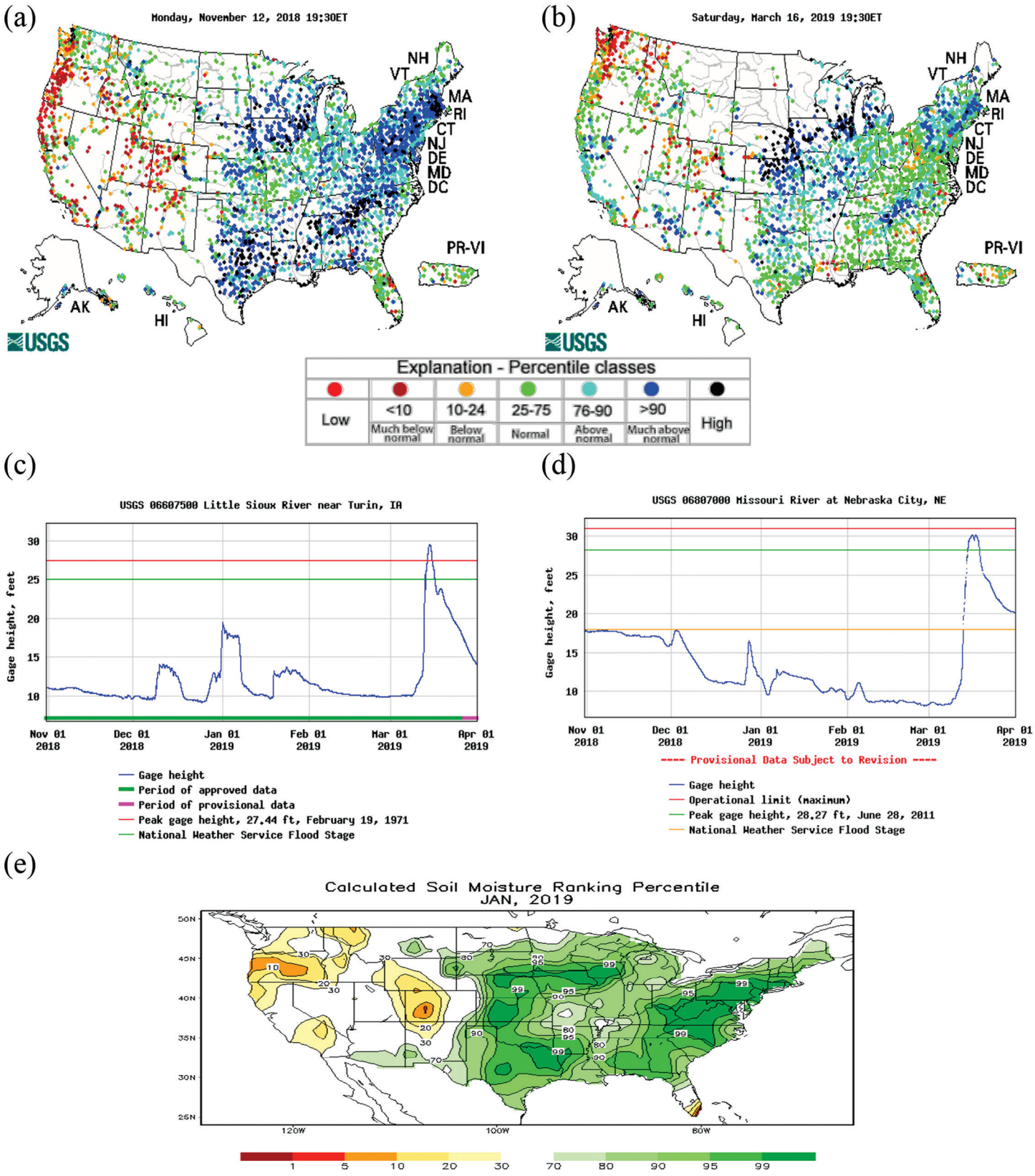

Fig. 2. U.S. Geological Survey (USGS) real-time streamflow for (a) 12 Nov and (b) 16 Mar 2019. The streamflow measurements are in percentiles based on the entire record of each station. Stations with under 30 years of coverage are not used. USGS gauge height (feet; 1 ft ≈ 0.306 m) readings on the (c) Little Sioux River near Turin, Iowa, and (d) Missouri River near Nebraska City from 1 Nov 2018 to 31 Mar 2019. USGS gauge data are available at https://waterdata.usgs.gov/nwis/rt. (e) The Climate Prediction Center Leaky Bucket Model modeled soil moisture percentiles for January 2019.

area. Prior to the event, National Weather Service (NWS) offices were forecasting and communicating the possibility of record-breaking floods across the study area. Ultimately, the Federal Emergency Management Agency (FEMA) declared a major disaster for both Nebraska and Iowa, with a preliminary damage estimate of at least $3 billion.

No single factor can explain the occurrence of this historic flood event. Hence, it is critical to understand how the combination of meteorological, climatological, and hydrological conditions led to large-scale flooding across the region. The purpose of this brief paper is to: 1) discuss the rapid cyclogenesis event and preceding surface and hydrological conditions across eastern Nebraska, western Iowa, and southeastern South Dakota; 2) examine how the synergy between these independent factors led to large-scale major flooding; and 3) investigate the forecast and communication of flood impacts across Nebraska, Iowa, and South Dakota.

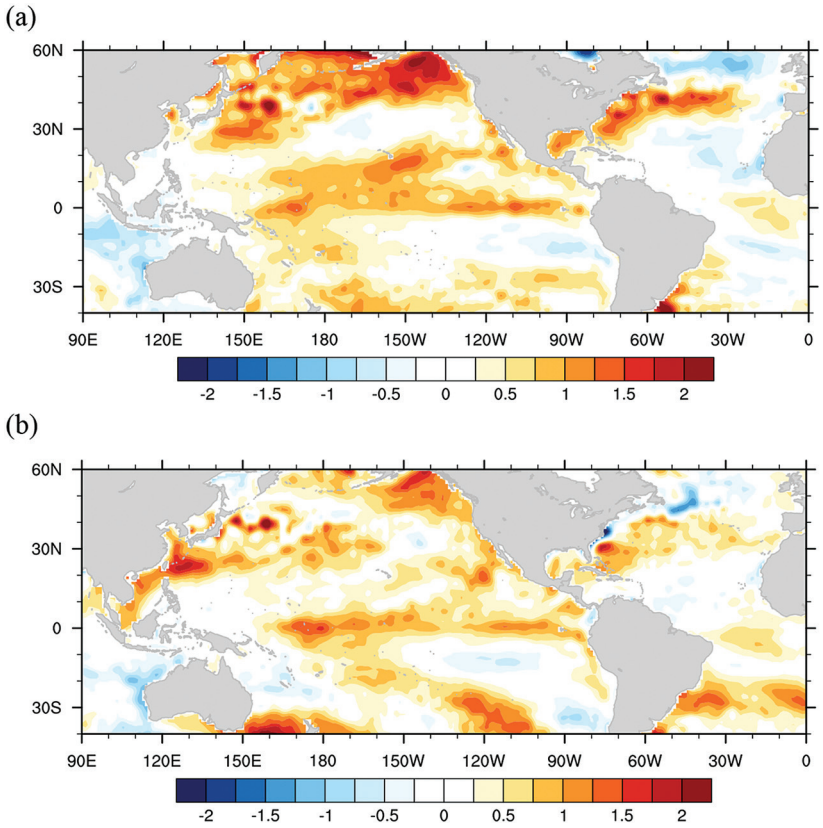

Fig. 3. NOAA Optimum Interpolation SST V2 anomalies (°C) for (a) September–November 2018 and (b) December 2018–February 2019. Anomalies were calculated using the 1981–2010 base period climatology.

Prior hydrometeorological context

During the 2018 fall (Fig. 3a) and 2018/19 winter (Fig. 3b) seasons, sea surface temperatures (SSTs) across the tropical Pacific were warmer than normal, (Fig. 3) indicating a developing El Niño event. These SST conditions increased the chances of a wetter winter season across the southern United States, near-normal moisture conditions in the study area, and a milder winter season across the northern United States, including most of the study area (CPC 2017). Additionally, the North Atlantic Oscillation (NAO) was positive during December and January (0.61 and 0.59), the Arctic Oscillation (AO) was weakly positive (December; 0.110) and negative (January; −0.713), and the Pacific–North American (PNA) teleconnection pattern was positive (0.86 and 0.83) (available at www.cpc.ncep.noaa.gov/products/precip/CWlink/pna/nao.shtml, www.cpc.ncep.noaa.gov/products/precip/CWlink/daily_ao_index/ao.shtml, and www.cpc.ncep.noaa.gov/products/precip/CWlink/pna/norm.pna.monthly.b5001.current.ascii.table, respectively). It is well known that the positive NAO would force slightly warmer temperatures over the central United States with little impact on precipitation (Hurrell et al. 2003), the weak AO would not largely impact the overall weather (Wang et al. 2005), and the positive PNA would drive warmer temperatures over the western and north-central United States (Leathers et al. 1991). The early part of the winter season (December 2018 and January 2019) was warmer and wetter relative to February and March in the study area (Fig. 4). Runoff from river systems were above average across most of the region (Fig. 2a) prior to freezing. Precipitation across the region was above normal (Fig. 4c), with average snowfall totals through the end of January at approximately 30.5 cm. Even so, because of the warmer early winter season temperatures

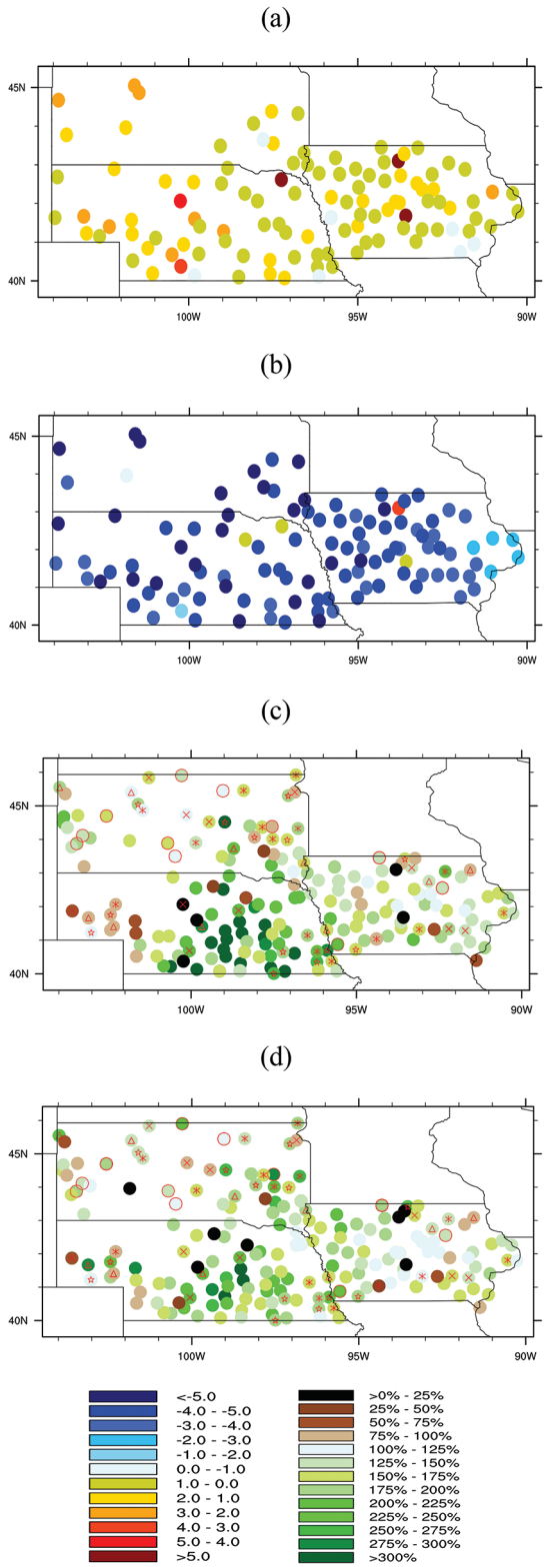

Fig. 4. Global Historical Climatology Network (GHCN) station (a) monthly surface daily temperature anomalies (°C) for December and January, (b) monthly surface daily average temperature anomalies (°C) for February and March 2019 , (c) monthly precipitation percentage of normal for December 2018 and January 2019, and (d) monthly precipitation percentage of normal for February and March 2019. Stations were filtered by length of record, with only stations having at least 50 years of data prior to 2019 being accepted into the analysis. Anomalies were calculated using the period of record for each station. Daily temperature averages were computed as an average between the maximum and minimum daily temperature averages for each month. Station 2018/19 snow season snowfall total records include a red symbol, with a circle representing a new record, a star is for a second-highest snowfall observation, three lines for a third-highest snowfall observation, two lines for a fourth-highest snowfall observation, and a triangle for a fifth-highest snowfall observation.

(Fig. 4a), no significant snowpack had developed by the end of January. Part of the moisture from the early winter season precipitation (either rain or snow) was absorbed by the land surface and as a result, soils were nearly saturated during this portion of 2019 (Fig. 2e). In January, temperatures across the study area had begun to decrease such that the soils were frozen by the end of the month.

It was also found that the center of the warm SST anomalies in the Pacific had shifted from the early to late winter. The primary center was now seen in the central tropical Pacific (Fig. 3b). This location of warm SST anomalies has been linked to increased chances of excessive precipitation over the south-central United States (Livezey et al. 1997; Flanagan et al. 2019). Further, these central Pacific warm SST anomalies are not associated with the typical higher chance of northern U.S. warming, observed during typical eastern tropical Pacific warm events (Ashok et al. 2007). The NAO continued to be positive during February and March (0.29 and 1.23), the AO became strongly positive (1.149 and 2.116), and the PNA shifted to negative (−1.08 and 0.25), with the month of March showing a positive PNA index owing to large (~0.5–1.3) positive daily PNA values after the cyclogenesis event. This is an interesting feature, as both positive NAO and AO would normally aid in keeping temperatures milder during the winter season over the central United States. As indicated above, this was not the case. The colder temperatures during February and March were caused by a persistent northwesterly flow regime over the northwestern and north-central United States due to ridging across the northwestern United States. The negative PNA regime can force such a pattern over this portion of the United States (Leathers et al. 1991). Thus, the cold temperatures were linked to the persistent negative PNA signal during this portion of winter 2019. Frigid temperatures occurred across the region from late January through March (Fig. 4b). This shift in temperatures finally caused rivers to freeze, with the Platte River having an ice depth around 43 cm (at Leshara, Nebraska). Further, with wet soils and lacking an insulating snowpack, the cold temperatures formed a deep and hard frost layer prior to March (Fig. 5a). With these cooler temperatures came a changeover of precipitation, as snowfall began to occur more frequently. The above-average precipitation resulted in numerous snowfall records being broken across the region (Figs. 4c,d), setting up a deep and moist snowpack (Figs. 5b,d). Approximately 10–20 cm of snow was observed across the region (Fig. 5b), with the snowpack showing around 3–10 cm of snow water equivalent (SWE; Fig. 5d). The frozen soil did not allow for infiltration of moisture from melted snow and expectations were that a rapid melting event would spell disaster for the region.

The Global Historical Climatology Network stations that show the season's top five snowfall records for 2018/19 are highlighted in Figs. 4c and 4d. It is to be noted that other stations within the region had "records" but did not pass the quality control checks we utilized to produce the station plots. In previous spring flood events, namely, 1881 and 1952, hydrometeorological conditions were similar to conditions of 2019. For the 1881 floods, 60–80 cm of river ice was reported and for the 1952 event, SWE values were around 8–13 cm along with saturated soils from wetter than average fall and winter seasons (NOAA 1954). Overall, the region was setup for a flood near or above the previous floods of record in the region. Early winter hydrological conditions, extreme cold and anomalous precipitation during the later winter put in place conditions ready for a rapid, significant flood event for the study region.

Rapid cyclogenesis of 12–14 March 2019

Reanalysis data from the National Centers for Environmental Prediction–National Center for Atmospheric Research (NCEP–NCAR), reanalysis, version 1 (Kalnay et al. 1996) were utilized to provide a synoptic overview of the event. The dataset is available from the Earth System Research Laboratory (ESRL) Physical Science Division (PSD) database (www.esrl.noaa.gov/psd/data/gridded). This 2.5° × 2.5° globally gridded dataset is updated daily, from 1948 to the present. Using this dataset, we analyzed sea level pressure (SLP); surface

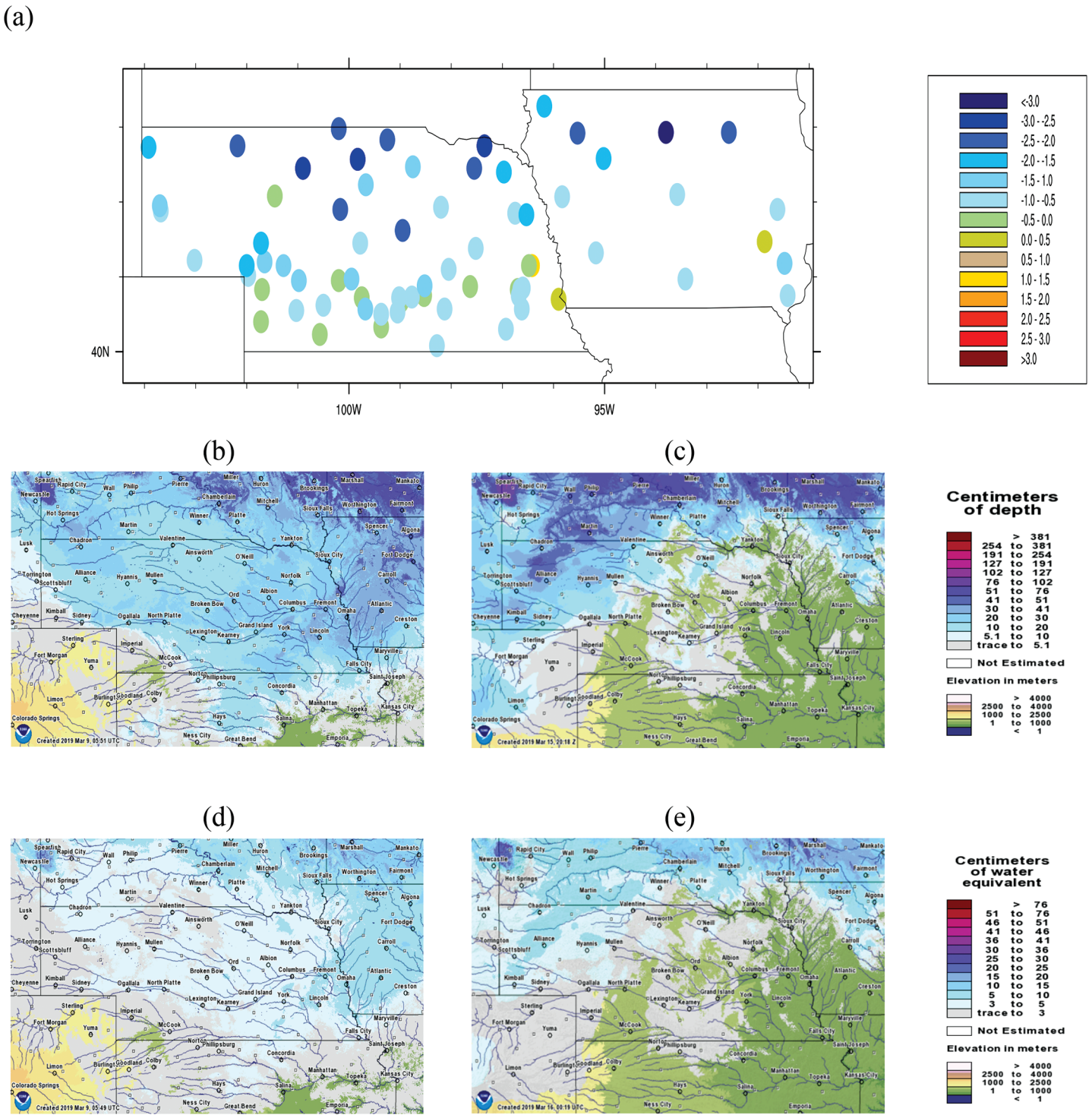

Fig. 5. (a) Automated Weather Data Network (AWDN) 7-day soil temperature (°C) observations for 6–12 Mar. National Operational Hydrologic Remote Sensing Center (NOHRSC) modeled snow depth (cm) for (b) 9 Mar and (c) 15 Mar 2019 and SWE (cm) for (d) 9 Mar and (e) 15 Mar 2019. Available at www.nohrsc.noaa.gov/.

temperature and winds; precipitable water; 250- and 500-hPa winds and geopotential heights; and 850- and 925-hPa winds, temperature, and heights using the NCAR Command Language (NCL; http://dx.doi.org/10.5065/D6WD3XH5). This dataset was utilized to derive all advection terms. Standardized anomalies were created for temperature, geopotential height, precipitable water, and SLP to present critical variables in the context of the time of year and regional climate. This was accomplished by using 21-day centered means from a 30-year base period (1981–2010) and standardized by the standard deviation, given by

$$\sigma_A = \frac{X - \mu}{\sigma}, \qquad (1)$$

where X is the observed gridpoint value, μ is the centered 21-day climatological mean, and σ is the standard deviation (Durkee et al. 2012).

On 12–13 March, a rapid surface cyclogenesis event took place across the central United States (Fig. 6). A closed trough across the southwestern United States propagated toward the north at the same time as a longwave trough shifted down from the north. These two systems began interacting late on 12 March, in the lee of the Rocky Mountains in eastern Colorado. As this area already had a low pressure zone near the surface (Fig. 6a), and owing to the converging troughs across the region (Figs. 6c,d), a rapid lee cyclogenesis event took place (Fig. 6b; American Meteorological Society 2019). This caused surface pressure values to plummet, leading to a record low pressure reading over eastern Colorado (970.4 hPa; NWS 2019a; Colorado Climate Center 2019) and Kansas (974.7 hPa; NWS 2019b), with a drop of 24 hPa (from 994 to 970 hPa) in 15 h on 12 March (NWS 2019c). This rapid lee cyclogenesis event was the primary driver of the excessive precipitation which occurred over the study region on 13 March.

However, prior to this cyclogenesis event, the gradient zone between the upper-level closed trough and the broad ridge over the eastern United States (Fig. 6c) caused southerly flow across a majority of the central United States (Fig. 7a). This caused warm, moist air to begin to advect over the central part of the country (Fig. 7b). As the cyclogenesis event began to take place, the advection regime strengthened, bringing an anomalously warm (Fig. 7c) and near record breaking deep moist air mass over the central United States (Fig. 7d). This is reflected in the record precipitable water values across the

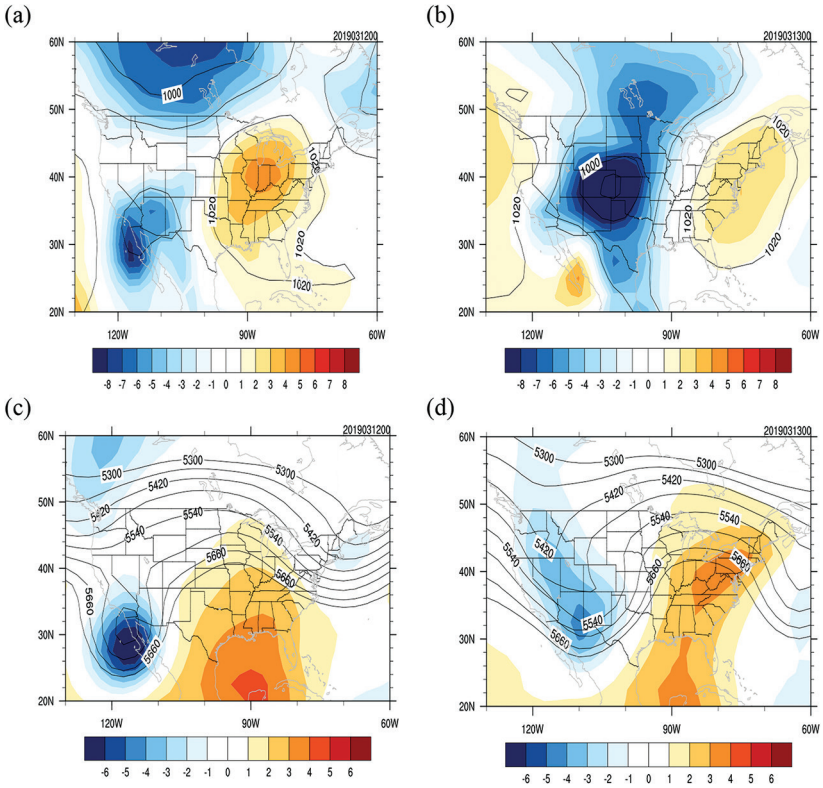

Fig. 6. NCEP–NCAR reanalysis daily averaged data for 12 Mar. (a) The daily averaged SLP (contours) and the standardized anomaly (color fill) for 12 Mar. Geopotential height contours go from 900 to 1,050 hPa with a 10-hPa interval and the standardized anomalies are color filled from –8 to 8 hPa with a 1-hPa interval. (b) The daily averaged SLP (contours) for 13 Mar. The contours for (b) are as in (a). (c) The daily averaged 500-hPa geopotential height (m; contours) and the standardized anomaly (m; color fill) for 12 Mar. Geopotential height contours from 5,300 to 5,700 m with a 60-m interval and the standardized anomalies are color filled from –6 to 6 m with a 1-m interval. (d) The daily averaged 500-hPa geopotential height (contours) and the standardized anomaly (color fill) for 13 Mar. The contours for (d) are as in (c).

region, with atmospheric soundings at Omaha, Nebraska (2.44 cm), and North Platte, Nebraska (1.80 cm), breaking their 0000 UTC 13 March records (2.159 and 1.37 cm, respectively) and Topeka, Kansas (2.57 cm), nearly breaking its record (2.62 cm) at 1200 UTC 12 March. Note that all of these soundings were taken prior to precipitation in their area. The advection of warm air resulted in rapid snowmelt that reduced the snowpack from a peak depth of 10–30 cm on 9 March to a trace on 15 March across most of eastern Nebraska and western Iowa (Figs. 5b,c). While temperatures were not high enough to cause large-scale snowmelt in southeastern South Dakota (Figs. 5b,c), temperatures were warm enough for the precipitation to fall as rain instead of snow (NWS 2019d). This can further be seen in the SWE figures (Figs. 5d,e), which show a rapid decrease across most of Nebraska and Iowa, while only extreme southeastern South Dakota saw a large decrease in snow coverage and the remainder of South Dakota maintained its snowpack. Thus, when rainfall began later on 12 March, runoff from prior snowmelt was already flowing into the region's streams and rivers. The excessive precipitation forced by the cyclone quickly caused rivers to rise to record-setting levels, overwhelming regional water storage infrastructure (Fig. 2b).

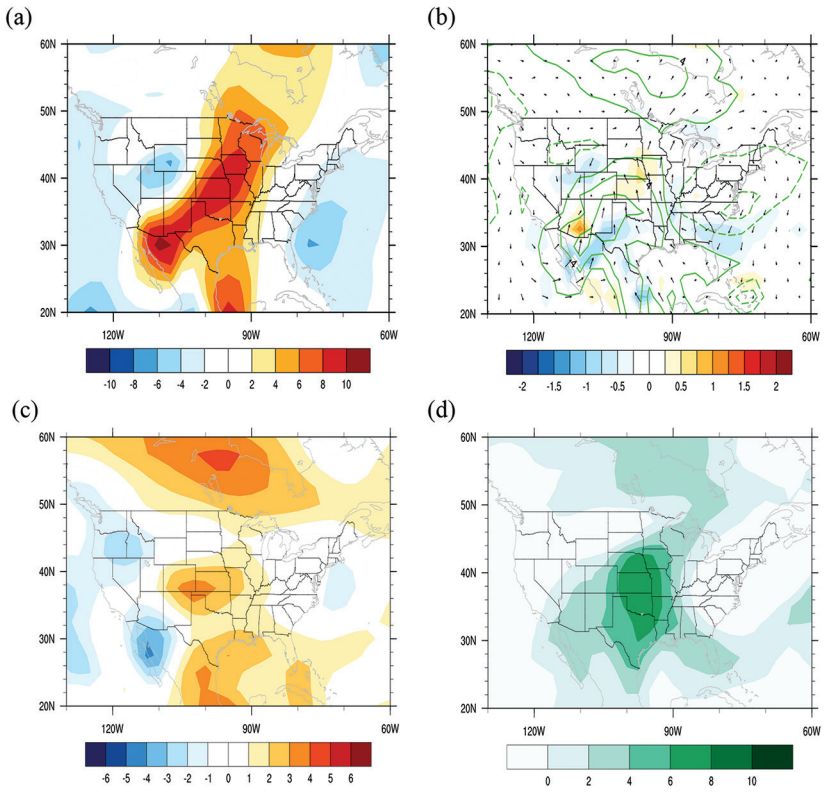

Fig. 7. NCEP–NCAR reanalysis (a) 925-mb υ-wind standardized anomalies (m s^{-1}). (b) The reanalysis 925-hPa moisture advection standardized anomalies (g kg^{-1} s^{-1}; shaded), specific humidity standardized anomalies (contoured from –12 to 12 g kg^{-1}; increment: 2 g kg^{-1}), and standardized anomaly vector wind (arrows). (c) The surface (1,000 hPa) temperature standardized anomalies (°C). (d) The precipitable water standardized anomalies (kg m^{-2}). Anomalies are from the 2-day period of 12–13 Mar 2019.

Flood forecast discussion

Prior to the event, the Weather Prediction Center (WPC) forecast approximately 50–75 mm in their 72-h quantitative precipitation forecast (QPF) from 0000 UTC 12 March to 0000 UTC 15 March (Fig. 8). The system was expected to efficiently produce precipitation from the anomalously moist air mass that was being advected into the area as the lee cyclone rapidly developed and propagated to the northeast.

Weeks prior to the flooding event, NWS Omaha/Valley officials were in communication with regional officials [emergency managers, Nebraska Emergency Management Agency (NEMA), etc.] and local media regarding the risk of flooding because of the extensive ice coverage of regional rivers (Nebraska Emergency Management Agency 2019). There were weekly ice jam update conference calls with core NWS Omaha/Valley partners and local media. The latter relayed flood potential and rainfall forecast information to stakeholders and local and state officials in the weeks leading up to the flood event. These conference calls disseminated the probabilistic risk of spring flood events, using information such as current streamflow percentiles, river ice status, and snowpack depth. As 12 March drew closer, clarity into the extreme nature of the event increased. A week prior to the flood event, NWS Omaha/Valley sent out

an updated spring flood outlook, which highlighted an increased threat for major flooding owing to the anomalous hydrological conditions throughout the area. When the model output precipitation forecast for 12–14 March started to take focus, local NWS offices began issuing flood watches for the region. Subsequently, these watches were updated to reflect the expected record-breaking nature of the event on the morning of 12 March over a large section of the NWS Omaha/Valley forecast area. These forecasts were supported by numerous observational (e.g., streamflow, river ice, and snowpack) and modeling resources (e.g., GEFS, ECMWF) including the ensemble situational awareness table (ESAT), which showed the potential for an extreme event a week prior to the flood event.

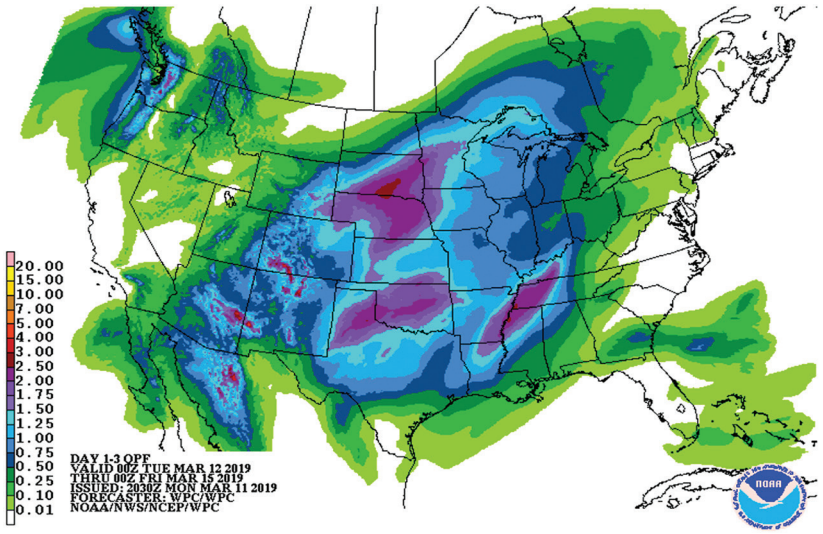

Fig. 8. WPC QPF forecast made on 11 Mar for the 72-h period beginning at 0000 UTC 12 Mar and ending at 0000 UTC 15 Mar.

The first round of precipitation came in the late afternoon on 12 March, but did not produce large-scale precipitation across the region as the forcing for ascent was weak at this time. Later, on 12–13 March, multiple rounds of precipitation came through the study area, as forecasted. Most areas in eastern Nebraska and western Iowa received around 12–25 mm of liquid precipitation with isolated areas reporting around 25–50 mm (Fig. 9a). However, areas farther west, mainly in the tributary region of the Platte River (e.g., the Loup and Wood Rivers) and in southeastern South Dakota, received 40–75 mm of primarily liquid precipitation on 12–14 March. Thus, the storm total precipitation amounts matched well with the WPC forecasted precipitation totals. At approximately 1400 UTC 14 March, precipitation began to cease in the study region due to a rapidly developing area of dry air forced by the occlusion process of the surface low. Farther west in Nebraska and South Dakota, snowfall began or continued to fall on the cold side of the occluding cyclone, causing blizzard conditions and producing around 15 cm of snow across most of the western portions of Nebraska and South Dakota (Fig. 9b). This snow would later melt and further exacerbate flood conditions across the region. Due to the existing snowpack and frozen soil conditions, almost all of this precipitation quickly ran into rivers and creeks. The large amount of water produced by the melting snow (Fig. 9c) and the excessive runoff from the liquid precipitation quickly overwhelmed the watersheds across the region and verified the NWS flood warnings.

Summary and perspective

During mid-March of 2019, the study area was impacted by record-setting floods. This flood event was triggered by precipitation forced by the record-low surface cyclone that rapidly developed across eastern Colorado and brought record daily precipitation amounts across portions of Nebraska, either through rain or the heavy snowfall. Preceding the flood event, weeks of anomalously low surface temperatures and accumulation of snow prior to the cyclogenesis event caused soil conditions that led to anomalously high runoff. In addition, warm advection and rainfall quickly melted the abnormally thick snowpack that blanketed most of the study region. Although the rapid cyclogenesis of the lee cyclone in eastern Colorado is typical for this time of the year (Petterssen 1956; Chung et al. 1976; Roebber 1984; Pierrehumbert 1986; Clark 1990; Schultz and Doswell 2000), this particular event produced a surface cyclone that

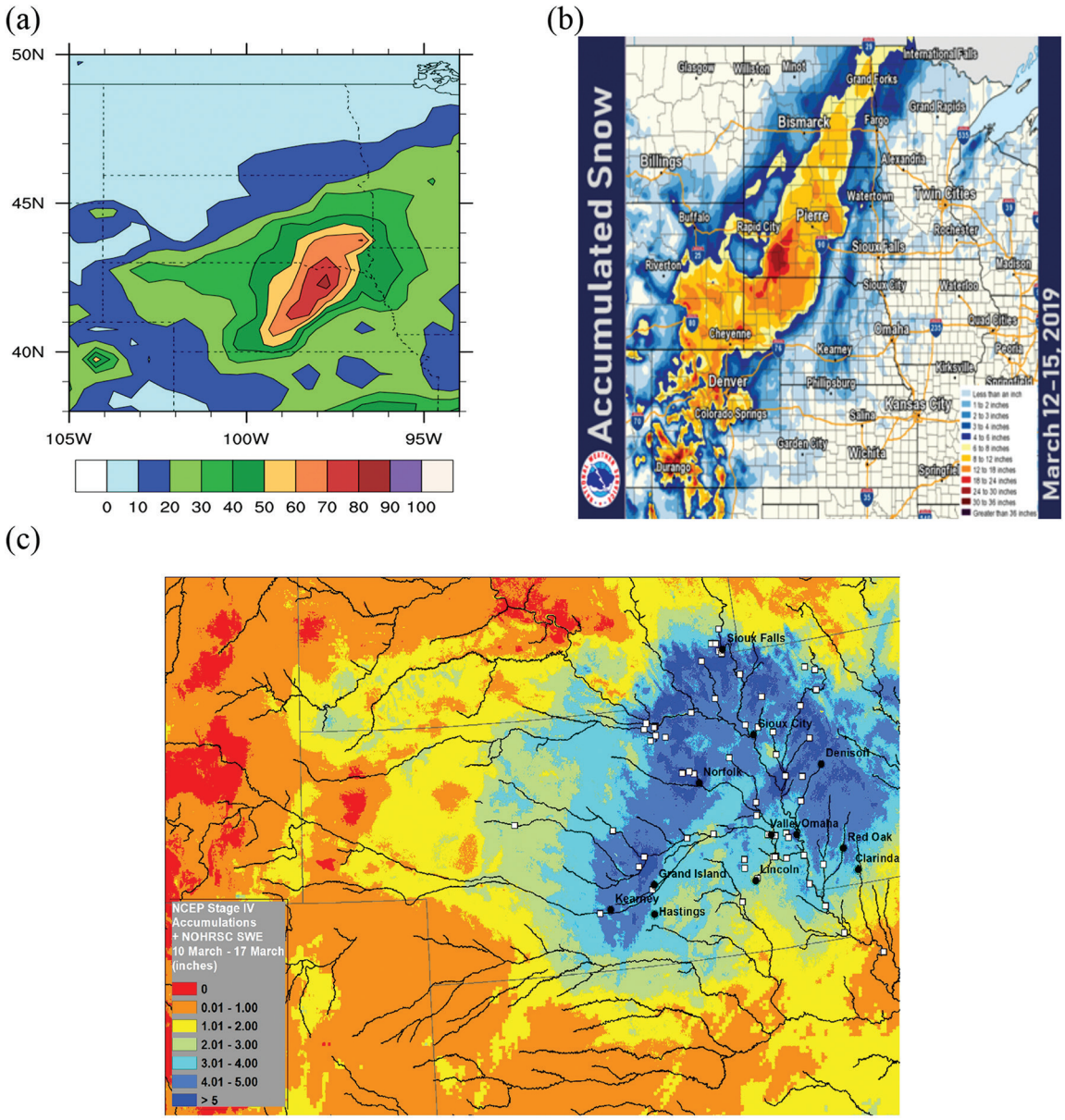

Fig. 9. (a) CPC Global Unified Gauge–based daily precipitation analysis (mm) for 12–14 Mar. (b) The accumulated snow (inches; 1 in. = 25.4 mm) for 12–15 Mar 2019. Available at www.weather.gov/fsd/20190314-Flooding. (c) The liquid precipitation and SWE totals for 10–17 Mar 2019. The liquid precipitation totals are from the NCEP Stage IV product and the SWEs are from the NOHRSC database. The white squares in (c) represent river gauges that set near-flood-stage records during the March flood event.

was more intense than any previously recorded in the Colorado and Kansas. Together, the record deep low pressure system and the anomalously moist air mass brought about 12–25 mm of precipitation over southeastern Nebraska and southwestern Iowa, 25–50 mm across northeastern Nebraska and northwestern Iowa, and 40–75 mm over large portions of central Nebraska and southern South Dakota. With the rapidly melting, moist snowpack and ice jams on the waterways, the precipitation quickly exceeded the channel flow capacity of rivers in the region and began the expansive flooding.

While not a focus of the research presented here, the authors believe the extensive and costly event highlights the current forecasting ability of the WPC QPF capabilities. Their forecasts weeks and days ahead of the primary and catastrophic flood event across the study

region provided much-needed warning far enough ahead of time that it likely saved numerous lives and personal property. This was aided by the probabilistic and deterministic forecasts which showed the heightened risk for an extreme weather event and subsequent flood a week before the cyclogenesis event occurred. Further, this successful forecast highlights the importance of extensive, high-spatial-resolution monitoring networks. Without the knowledge of the frozen soils and large snowpack across the region, local NWS offices would have lacked crucial information into the scale and magnitude of the flood event that took place. Further, this event established far above normal hydrological conditions throughout the study region, that is, the Missouri River basin. After the flood event in March, meteorological and hydrological conditions have been such that the region is still completely saturated heading into the 2019/20 winter season, meaning that river levels are largely above normal and soil moisture levels are at or near capacity. Further, owing to the above-average water conditions throughout the Missouri River basin, heavy precipitation events throughout 2019 caused rapid flood events, especially in southeastern South Dakota. It would be remiss not to note that the flood event of March 2019 helped to developed extreme hydrologic conditions across Nebraska, Iowa, and South Dakota that are conducive for further flood events in 2020. Lastly, this event underscored the importance of communication between forecasters and local/regional stakeholders, local officials, and the media. This allowed NWS officials to disseminate crucial flood forecast information to "key players" rather than using the time prior to the event searching for "the right people to talk to."

Acknowledgments. NCEP–NCAR reanalysis data were obtained from the NOAA/ESRL Physical Sciences Division, Boulder, Colorado, from their website at www.esrl.noaa.gov/psd/data/gridded. CPC Global Unified Precipitation data are provided by the NOAA/OAR/ESRL PSD, Boulder, Colorado, from their website at www.esrl.noaa.gov/psd/. We thank NCAR for the NCAR Command Language (version 6.2.1), UCAR/NCAR/CISL/TDD, Boulder, Colorado, http://dx.doi.org/10.5065/D6WD3XH5.

References

American Meteorological Society, 2019: Lee cyclogenesis. *Glossary of Meteorology*, accessed 29 July 2019, http://glossary.ametsoc.org/wiki/Lee_cyclogenesis.

Ashok, K., S. K. Behera, S. A. Rao, H. Weng, and T. Yamagata, 2007: El Niño Modoki and its possible teleconnection. *J. Geophys. Res.*, **112**, C11007, https://doi.org/10.1029/2006JC003798.

Chung, Y.-S., K. D. Hage, and E. R. Reinelt, 1976: On lee cyclogenesis and airflow in the Canadian Rocky Mountains and the East Asian mountains. *Mon. Wea. Rev.*, **104**, 879–891, https://doi.org/10.1175/1520-0493(1976)104<0879:OLCAAI>2.0.CO;2.

Clark, J. H. E., 1990: An observational and theoretical study of Colorado lee cyclogenesis. *J. Atmos. Sci.*, *47*, 1541–1561, https://doi.org/10.1175/1520-0469(1990)047<1541:AOATSO>2.0.CO;2.

Colorado Climate Center, 2019: Storm records. Accessed 9 December 2019, https://climate.colostate.edu/pdfs/storm_records.pdf.

CPC, 2017: El Niño and La Niña–Related winter features over North America. NOAA, accessed 22 August 2019, www.cpc.ncep.noaa.gov/products/analysis_monitoring/ensocycle/nawinter.shtml.

Durkee, J. D., L. Campbell, K. Berry, D. Jordan, G. Goodrich, R. Mahmood, and S. Foster, 2012: A synoptic perspective of the record 1–2 May 2010 mid-South heavy precipitation event. *Bull. Amer. Meteor. Soc.*, **93**, 611–620, https://doi.org/10.1175/BAMS-D-11-00076.1.

Flanagan, P. X., J. B. Basara, J. C. Furtado, E. R. Martin, and X. Xiao, 2019: Role of sea surface temperatures in forcing circulation anomalies driving U.S. Great Plains pluvial years. *J. Climate*, **32**, 7081–7100, https://doi.org/10.1175/JCLI-D-18-0726.1.

Hurrell, J. W., Y. Kushnir, G. Ottersen, and M. Visbeck, 2003: *The North Atlantic Oscillation: Climate Significance and Environmental Impact, Geophys. Monogr.*, Vol. 134, Amer. Geophys. Union, 279 pp.

Kalnay, E., and Coauthors, 1996: The NCEP/NCAR 40-Year Reanalysis Project. *Bull. Amer. Meteor. Soc.*, **77**, 437–471, https://doi.org/10.1175/1520-0477(1996)077<0437:TNYRP>2.0.CO;2.

Leathers, D. J., B. Yarnal, and M. A. Palecki, 1991: The Pacific/North American teleconnection pattern and United States climate. Part I: Regional temperature and precipitation associations. *J. Climate*, **4**, 517–528, https://doi.org/10.1175/1520-0442(1991)004<0517:TPATPA>2.0.CO;2.

Livezey, R. E., M. Masutani, A. Leetmaa, H. Rui, M. Ji, and A. Kumar, 1997: Teleconnective response of the Pacific–North American region atmosphere to large central equatorial Pacific SST anomalies. *J. Climate*, **10**, 1787–1820, https://doi.org/10.1175/1520-0442(1997)010<1787:TROTPN>2.0.CO;2.

Nebraska Emergency Management Agency, 2019: By the numbers–Nebraska's historic floods. NEMA News Release, 3 pp., https://nema.nebraska.gov/sites/nema.nebraska.gov/files/press/doc/NEMA%20AM%20NewRelease%203.17.19.pdf.

NOAA, 1954: Floods of 1952 Upper Mississippi–Missouri–Red River of the North. Tech. Rep. 23, 101 pp, www.nws.noaa.gov/oh/hdsc/Technical_papers/TP23.pdf.

NWS, 2019a: March 13th and 14th, 2019 Bomb Blizzard. Accessed 29 July 2019, www.weather.gov/cys/March13142019Blizzard.

——, 2019b: Historic low pressure system affects the Plains! Accessed 9 December 2019, www.weather.gov/ict/event_20190313.

——, 2019c: Mid-March 2019: Historical, catastrophic flooding impacts parts of central/south central Nebraska. Accessed 29 July 2019, www.weather.gov/gid/march2019flood.

——, 2019d: Heavy rain and snow melt create widespread flooding – March 13-14, 2019. Accessed 15 November 2019, www.weather.gov/fsd/20190314-Flooding.

Petterssen, S., 1956: *Motion and Motion Systems*. Vol. I, *Weather Analysis and Forecasting*, McGraw-Hill, 428 pp.

Pierrehumbert, R. T., 1986: Lee cyclogenesis. *Mesoscale Meteorology and Forecasting*, P. S. Ray, Ed., Amer. Meteor. Soc., 493–515.

Roebber, P. J., 1984: Statistical analysis and updated climatology of explosive cyclones. *Mon. Wea. Rev.*, **112**, 1577–1589, https://doi.org/10.1175/1520-0493(1984)112<1577:SAAUCO>2.0.CO;2.

Schultz, D. M., and C. A. Doswell III, 2000: Analyzing and forecasting Rocky Mountain lee cyclogenesis often associated with strong winds. *Wea. Forecasting*, **15**, 152–173, https://doi.org/10.1175/1520-0434(2000)015<0152:AAFRML>2.0.CO;2.

Wang, D., C. Wang, X. Yang, and J. Lu, 2005: Winter Northern Hemisphere surface air temperature variability associated with the Arctic oscillation and North Atlantic oscillation. *Geophys. Res. Lett.*, **32**, L16706, https://doi.org/10.1029/2005GL022952.